GEOFIZIKA VOL. 29 2012

Original scientific paper
UDC 551.521.18

Near infrared light pollution measurements in Croatian sites

Željko Andreić [1, 3], *Doroteja Andreić* [2, 3] *and Krešimir Pavlić* [1]

[1] University of Zagreb, Faculty of Mining, Geology and Petroleum Engineering, Zagreb, Croatia

[2] University of Zagreb, Faculty of Veterinary Medicine, Zagreb, Croatia

[3] Višnjan Observatory, Višnjan, Croatia

Received 3 November 2011, in final form 31 May 2012

We investigate the light pollution (LP) in the near-infrared (NIR) part of the electromagnetic spectrum (700–1000 nm) for sites at low altitude, as typical for small observatories in this region. Our measurements show that considerable light pollution exists in the NIR. The increase of night sky brightness towards the horizon is often slightly slower in the NIR than in the visible. In cases when LP is mostly produced by high-pressure sodium lamps, the NIR part of light pollution is dominated by two close sodium spectral lines (818.3 and 819.5 nm) that can easily be filtered out with a dedicated filter. This can, however, change as sodium lamps are gradually replaced by metal-halide lamps whose spectra are complex, showing many lines over the whole visible/infrared range. If in the future a change to LED light sources happens, LP in the NIR could be reduced drastically. Last, but not least, the low altitude of observing sites, together with climate characteristics of the region, result in a lot more humidity and aerosols in the atmosphere, compared to a typical mountaintop observatory site. This, combined with proximity of the polluting sources to the observing sites, results in enhancing the LP, compared to the clear, dry atmospheric conditions of a mountaintop observatory.

Keywords: light pollution, infrared: general

1. Introduction

Light pollution is defined as any artificial light that escapes into the environment, and as such, it is related to the human vision. Astronomically, only the effect of increased night sky brightness is considered to be the light pollution. Today, however, most observations are carried out with some sort of silicon image sensors (CCD, CMOS, etc.). We may accordingly expand the definition of „light pollution“ to the whole spectral region to which such sensors are sensitive, approximately from 350 to 1100 nm.

The light pollution is a severe problem for small observatories. Such observatories are usually located near, or even in the middle of large towns and LP at their sites is often severe. Most of these locations are also at low altitudes so the amount of water vapor and aerosols in the atmosphere can be tenfold or more larger than at remote mountain sites typical of large observatories.

Both the Rayleigh scattering coefficient and the aerosol scattering coefficient drop significantly with the wavelength (RCA, 1978). Rayleigh coefficient drops by a factor 16 when wavelength is increased from 500 to 1000 nm, and the aerosol scattering coefficient drops by a factor of 1.5, which gives hope for a better signal to noise ratio (SNR) for observations at NIR wavelengths, compared to the observations in visible, in cases when a significant amount of LP is present. On the other side, natural sky emissions are at least an order of magnitude stronger in the NIR, compared to the visible, with the effect that more LP is needed to produce the same relative increase of background brightness as in the visible.

In this paper we describe studies carried out at low altitude observing sites which have considerable amounts of LP. Such sites are typical for our region, the nearest sites with near-natural sky being at least one day travel away. Similar studies were carried out in the visible (Duriscoe et al., 2007; Falchi, 2011), but, to our knowledge, none were done in the NIR so far.

2. Observations

The distribution of the night sky brightness over the celestial hemisphere was measured with a modified digital camera (Canon EOS 300D). In this camera, the UV-IR blocking filter is replaced by a clear quartz glass window, so that the full spectral range to which the C-MOS detector of the camera is sensitive, can be exploited. The selection of smaller spectral regions is realized by use of different filters, placed in the optical path in front, or immediately behind, the camera lens. In our case two filters were used: an UV-IR blocking filter which transmits visible light between 380 and 700 nm (Marumi, 2010), which is very similar in characteristic to the filters that are used in off-the-shelf digital cameras modified for astronomical use (Baader, 2010a,b). The difference to a standard digital camera filter is that the red sensitivity of a modified camera is maximized for H-α spectral line, while the sensitivity of „normal“ cameras to this wavelength is about 24% (Baader, 2010b).

The second filter used is an infrared-transmitting glass filter (Schott RG 830) which is a so-called edge filter that blocks all wavelengths below 800 nm and fully transmits above 860 nm (Schott, 2010). In this case the IR spectral response of the camera is set by the infra-red response of the camera chip itself.

The relative spectral sensitivity of the setup in both spectral windows is shown on the Fig. 1.

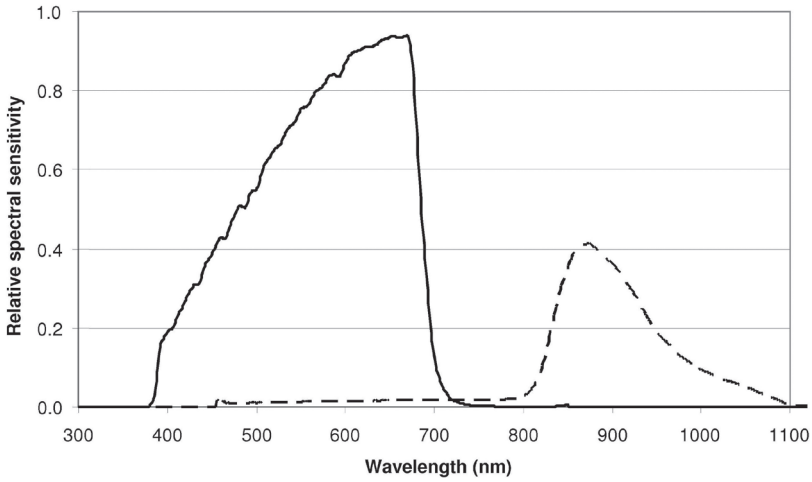

Figure 1. Relative spectral sensitivity of the modified EOS 300D digital camera in combination with Marumi UV-IR cut filter (solid line) or Schott RG-830 filter (dashed line). The original UV-IR cut filter of the camera is replaced by a quartz window.

Peleng fish-eye lens (8 mm F/3.5, closed to F/4) (Zenit, 2010) was used for all-sky photography. This lens produces an all sky image of 23 mm in diameter, that fits well to the standard 35 mm film format. However, on a digital camera, that generally has a smaller sensor (the camera we used has an APS-C sensor with size of 15.1 × 22.7 mm), the circle gets cropped at the longer sides of the image, the maximum cropping being about 30° from the horizon. We exploited this cropping effect to eliminate strong light sources near the horizon and prevent strong circular reflections they would produce in the image. The full 180° field of view is still preserved along the longer chip side. We also used a 5 mm high circular lens hood to mask the whole horizon up to the height of about 10°, to eliminate strong light sources when they were all around the observing site (as was the case in examples on Figs 3 and 4).

Typical exposures used in such a setup are 2–5 minutes at ISO 800 and F/4. The native raw image format was used to store images on the camera's memory card, thus providing 12-bit data resolution per color channel, compared to the 8-bit resolution of jpeg format that such cameras utilize. Dark and bias frames were taken between the light frames, or immediately after them.

The raw images were afterwards processed on a PC with the help of IRIS software (IRIS, 2010) in the usual way. The flat-field correction was done with the help of a synthetic flat field image. We had to choose this approach as we found no means to accurately flat-field our fish-eye lens. The vignetting function we used to create the synthetic flat field image was determined by measuring the brightness of image of a stable light source at various off-axis angles. It is shown on the Fig. 2.

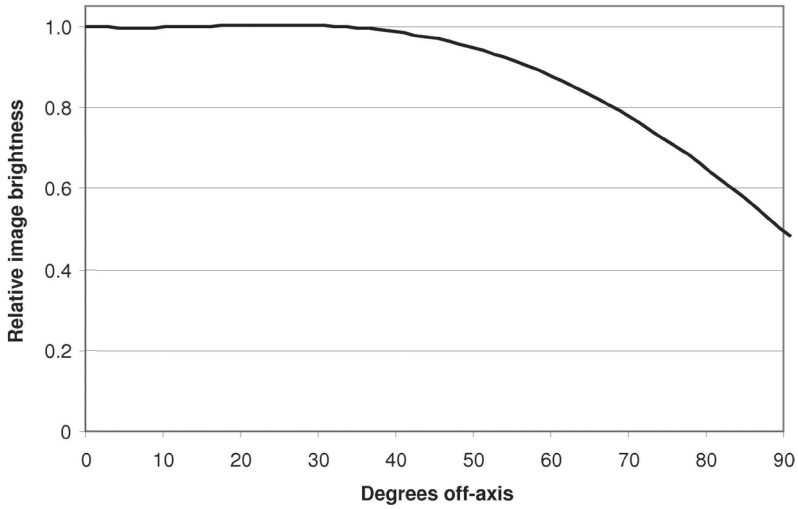

Figure 2. Vignetting of the 8 mm F/3.5 Peleng fish-eye lens.

The night sky spectra were taken with a small prismatic spectrograph of our own construction, which attaches directly to the digital camera. Usually, the spectrograph is directed towards the zenith and all radiation coming from the sky that enters into the acceptance angle of the instrument (FWHM = 13°) contributes to the spectrum. In such an arrangement the detector records the average spectrum of radiation coming from that part of the sky. The advantage of such recording technique is that the contribution of individual stars is diluted so much that, usually, it cannot be detected at all. Also, no tracking is required. The slit width was kept constant at 20 μm (the spectrograph camera magnification is 0.40). The relative spectral sensitivity of the instrument was measured by averaging solar spectra taken on several occasions, taking care that atmospheric condition is near standard one and that the Sun was at approximately same zenith distance, and comparing the results with a standard solar spectrum, corrected for the appropriate air-mass (ASTM, 2011). Additionally, the relative spectral sensitivity was modeled taking into account the relative spectral sensitivity of the camera sensor, variable spectrograph dispersion and glass transmittance. The comparison of the results allowed us to judge the accuracy of the spectral sensitivity curve we obtained. Except at extreme limits of observable spectral band, uncertainty in relative spectral sensitivity was found out to be less than ±7%.

The sky brightness at zenith was measured by the Sky quality meter (Unihedron, 2010a), model SQM-L. This instrument recently became very popular among amateurs and is now used worldwide. The difference between the basic model SQM (Unihedron, 2010b), and the „-L“ variant of the instrument is that SQM-L has a lens in front of the detector that reduces its angular sensitivity,

compared to the basic SQM model. The FWHM of the acceptance cone of the SQM-L is 20°, compared to 85° of the SQM. Although the measurements are in the standard units of magnitude per square arc second, the spectral sensitivity of the instrument differs considerably from the standard photometric „V" band (Cinzano, 2005) and is actually a close match to the sensitivity of a typical off-the-shelf digital camera. Cinzano suggests that the „SQM" photometric class should be introduced to settle this discrepancy (Cinzano, 2005).

Finally we disassembled one SQM-L device and removed its internal IR-blocking filter. Consequently, one has to use external filters to limit its sensitivity to the spectral region of interest, and calibration is lost, unless the original filter (Hoya CM-500,1 mm thick, (Cinzano 2005)) is used. However, the reproducibility and relative values of the measurements are preserved, so the device can still be used to characterize different locations, or different nights at the same location, in the spectral region of interest. This can be useful to someone who images only in the NIR, for example. Also, due to the 20° FWHM, it is possible to make crude estimate of the night sky brightness distribution. To test this idea, we occasionally made a few measurements of the night sky brightness at zenith distances of 0°, 15°, 30°, 45°, 60° and 75°, using a CM-500 or a RG 830 glass filter in front of the modified instrument.

3. Results and discussion

During the last 8 years we systematically studied LP conditions at a dozen sites in continental Croatia and at a few sea-side (Adriatic Sea or near its coast) sites. Each site was visited at least a few times. Most of them are at low altitude (0–300 m above sea level), and the highest site we studied is at 650 m above sea level. Infrared studies have been started 5 years ago. The sites were categorized according to the Bortle scale (Bortle 2001) which is in common use among amateurs and operators of smaller observatories. The IAU scale (IAU, 2012) is too strict and applies only to the almost perfect natural sky. This scale is not applicable to the most places we studied, as they all fall into the worst class C of this scale, making no distinction between them. On the other hand, the Bortle scale covers full range of levels of LP, from none to extreme, allowing easy distinction between places with different amounts of LP.

Climatologically, continental Croatia has temperate humid climate with warm summer (Cfb). Sites at northern Adriatic coast have temperate humid climate with hot summer (Cfa), and the rest of Adriatic area has Mediterranean climate with hot summer (Csa) (Wiki, 2011; Šegota and Filipčić, 2003). Concerning astronomical observations, a significant percentage of clear nights is humid, often with dew formation on exposed optical surfaces, especially in the spring and autumn. 30–50% of infrared all-sky images show presence of thin cirrus clouds, that are undetectable both visually and in the images taken in the visible. This has to be taken into account during planning of infrared observations. The

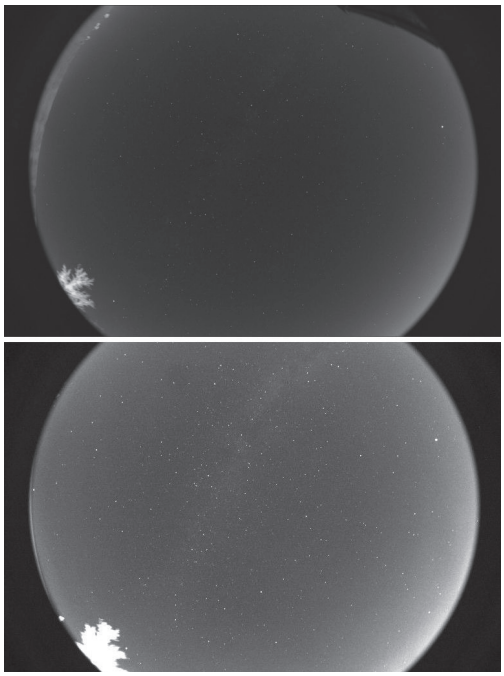

Figure 3. Moderately light-polluted sky (SQM-L zenith brightness 20.4 mag/arcsec^2) in visible (*top*) and in the NIR (*bottom*).

aerosol load of the atmosphere is often quite high, especially in summer. This is related not only to the climatology of the area, but also to the fact that the whole region is significantly populated. Although large areas of preserved nature do exist, the nearest settlement is usually just a few kilometers away, and a larger city is always nearer than 100 or so kilometers from any observing site one may find.

An example of all-sky image of a moderately polluted sky (Bortle class 6, see Bortle, 2001) is shown on the Fig. 3 (top). The picture was taken in the visible. The sky brightness at the zenith was about 1.5 mag above the natural night sky brightness (21.9 mag/arcsec^2, (Albers and Duriscoe, 2001)). The corresponding infrared image, taken immediately after the visible one (Fig. 3, bottom) clearly shows that the Milky Way is more prominent in the NIR image. This indicates that light pollution is less severe in the infrared, compared to the visible, a fact that is often exploited by amateur astronomers who cannot move to a better location.

The photometric analysis additionally shows that LP growth towards the horizon is a little slower than in the visible (Fig. 4). Results obtained on different nights and on several other locations with the approximately the same level of

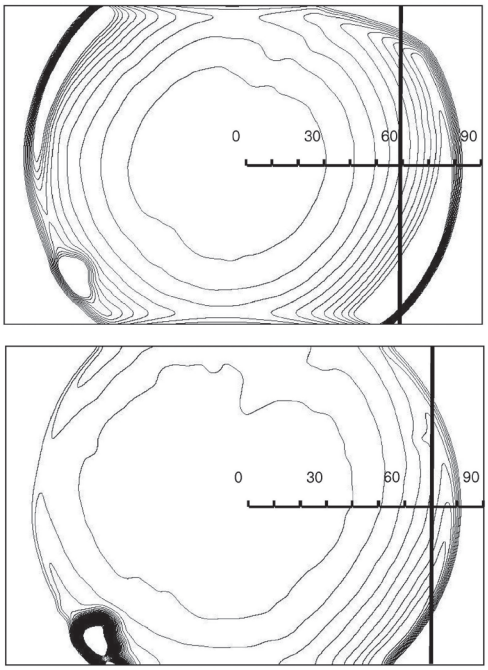

Figure 4. Isophotes derived from visible and NIR pictures of the moderately light-polluted sky. The isophote step is 20% of sky brightness at the zenith in both cases. The horizontal scale is zenith distance, and the vertical bar goes through the 100% increase isophote in both cases.

light pollution are similar to this. This can be explained by smaller Rayleigh aerosol scattering coefficients, compared to the visible, with the effect of less infrared scattered light returning down as light pollution. Also, current light sources produce far less infrared radiation compared to the visible, so LP in the infrared is lower due to this fact too.

3.1. SQM measurements

Tests carried out with modified SQM-L instrument show faster increase of light-pollution towards the horizon than data derived from all-sky images. We attribute this discrepancy to relatively large acceptance angle of the SQM-L, with the effect that the brighter sky in the lower part of the entrance cone contributes more to the total amount of radiation measured. This is supported by the fact that this apparently faster increase of the night sky brightness appears at large zenith angles. At small angles, the results are almost the same as those obtained by the isophote method.

The SQM-L data confirm slower growth of the LP towards the horizon in the infrared, compared to the visible (Fig. 5). However, the SQM-L measurement at

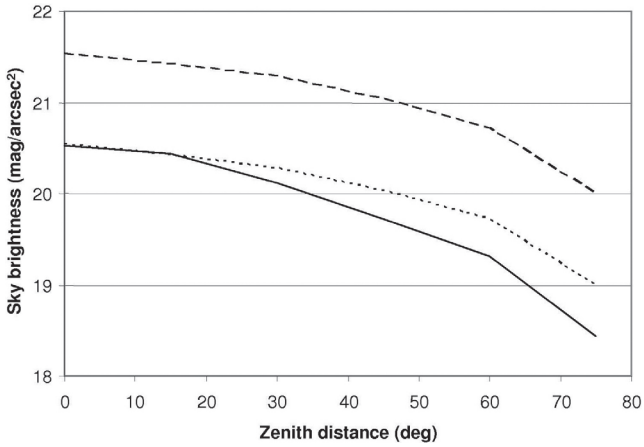

Figure 5. Sky brightness measured with a modified SQM-L device in visible (*solid line*) and IR (*dashed line*). The dotted line, overlapping the visible measurements, represents IR measurements with an offset of –1.0 mag, to ease the comparison of brightness growth towards the horizon.

high zenith angles can easily be spoiled by direct light from sources at horizon entering the sensitivity cone of the instrument, so care should be taken to avoid measuring in approximate direction of bright sources.

As we stressed before, infrared magnitude scale is not calibrated in absolute units, but relative measurements are still valid. This, and the difference in absolute sky brightness in visible, and in the infrared explain the relative shift of the SQM-L visible and infrared brightness curves presented on the Fig. 5.

3.2. The night sky spectrum

The low dispersion spectrum of the light polluted sky near zenith (Fig. 6, top) resembles closely the spectrum of high-pressure sodium lamps. This type of lamps is dominant in the public lighting around the site where the spectrum was taken. The visible part of the spectrum is dominated by pressure-broadened sodium D doublet, with the characteristic self-absorption at 589 nm, and several lines between 500 and 570 nm. Such a spectrum is almost impossible to filter-out even with sophisticated interference filters. Conversely, the near-infrared part of the spectrum is relatively free from light pollution, apart from a very strong sodium doublet at 818.3 and 819.5 nm, produced by the same lamps that pollute the visible spectrum. This line can easily be filtered out even with a simple stack of two relatively cheap glass filters (for instance, a stack of Schott KG3 and RG610 glass filters (Schott, 2010) transmits between 610 and 800 nm and blocks everything else), or observations can be made on the long wavelength side of this doublet, for instance by using a RG850 glass filter. In this case, however, the sensitivity of the camera chip is relatively small, thus exposures have

to be prolonged considerably (by a factor of 2-5, depending on the object and particular infrared filter used).

As a comparison, the spectrum of natural night sky (Fig. 6, bottom) is quite different, and is dominated by a few lines in the visible and broad, weak, molecular bands in the NIR. The most prominent lines are neutral oxygen lines at 558, 600 and 636 nm. The „line“ at 660 nm and weaker bands at longer wavelengths are all OH emission bands (Walker and Schwarz, 2007). A trace of high-pressure sodium lamp spectrum can be found between the green and red oxygen lines, but it is quite weak. This spectrum resembles night sky spectra obtained at large professional observatories, naturally, allowing for the large difference in spectral resolution (Walker and Schwarz, 2007; Patat, 2003). An example of a true natural sky spectrum in much better resolution is given on the Fig. 7. It is based on data compiled by the LSST team (Ivezić, 2011).

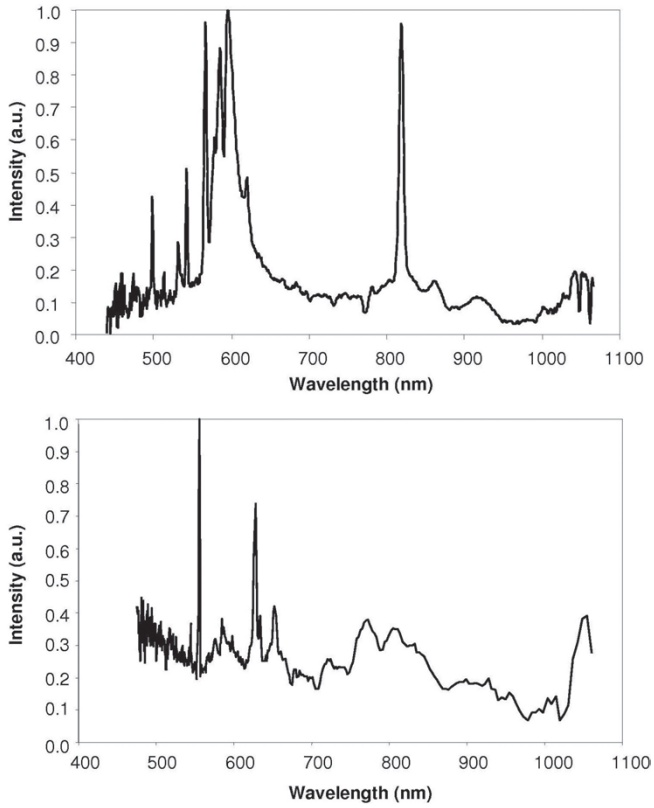

Figure 6. The spectrum of the light-polluted sky (*top*) and the spectrum of the natural night sky (*bottom*), both in arbitrary units. The natural sky spectrum is about 6 times weaker than the light polluted one.

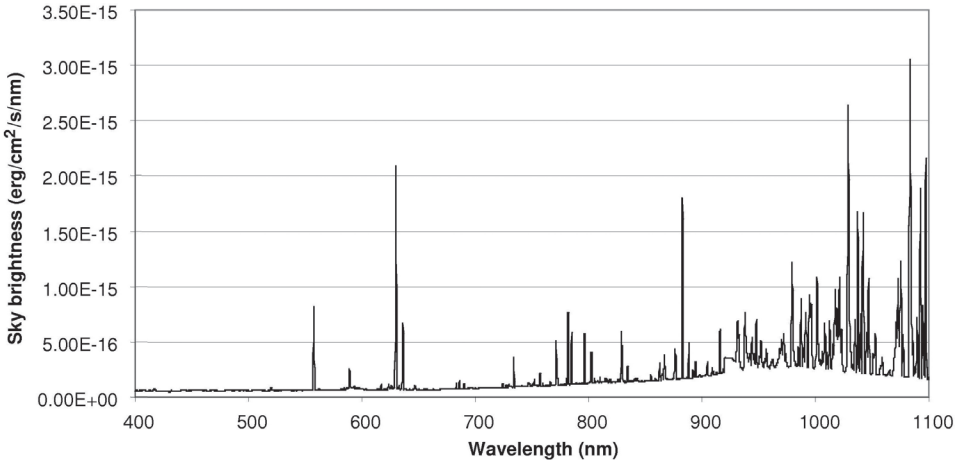

Figure 7. A compilation of observed sky emission spectra at various sites, as used in LSST simulations.

A word of caution must be spoken here. During 8 years of our studies most LP was generated by the high-pressure sodium lamps, with some percentage of mercury-vapor lamps still present in a few isolated areas, but their contribution was not significant, based on the night sky spectra. Recently, a newer kind of lamps, the so called metal-halide lamps are replacing high-pressure sodium lamps in public lighting systems. They have complex spectra with a lot of lines, both in the visible and in the infrared. Moreover, the spectra of different lamp types can be quite different from each other. This can worsen the problem of light pollution, especially in the infrared, as, due to the variable LP spectrum, there will be no easy way to filter it out.

One can notice that the objects on the horizon appear much brighter on infrared images than on corresponding visible ones. This is actually well known fact from infrared photography: most common objects have larger reflection coefficients in the infrared, especially green plants. Thus the trees and grass are usually quite dark on the visible, and very bright (so called „snow" effect) on the infrared images. As a consequence, the contribution of artificial light scattered from the ground to the light pollution is larger than in the visible. One should here take into account that at low altitude sites the scattering in the lower atmosphere is considerable, compared to the situation of mountain-top observatories, thus more than compensating for a smaller scattering coefficient in the infrared.

3.3. Situation at sites with different levels of LP

The effect of different strength of LP at various sites can be seen on the Fig. 8. We found that our conclusions hold for all sites with moderate and strong light

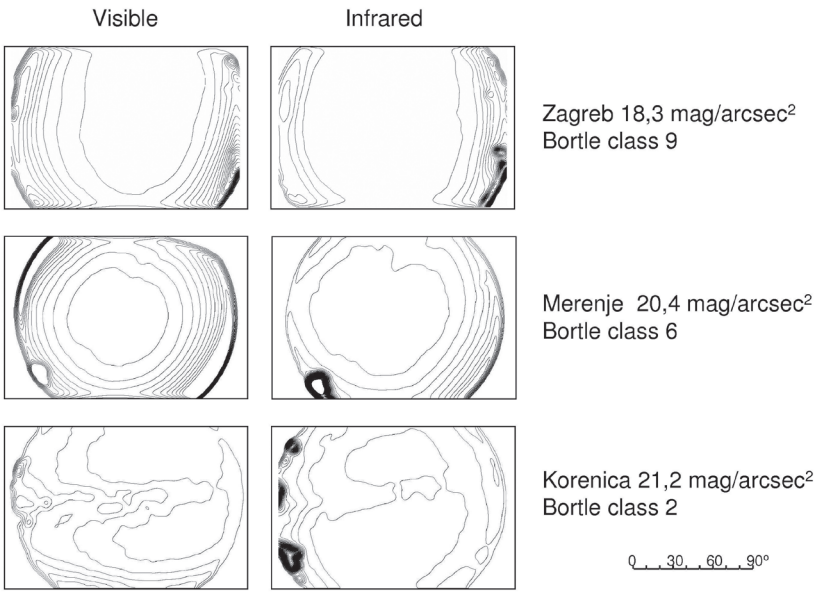

Figure 8. Isophotes of LP in the visible and in the near infrared at sites with various strengths of light pollution. In all cases isophotes are given for each 20% of increase of sky brightness compared to the brightness at the zenith.

pollution. Only at sites with very low levels of LP, when natural levels of sky brightness are comparable to, or larger than LP contribution, we see the effects of stronger natural emissions in the NIR, but even then the growth of sky brightness towards the horizon is slower than in the visible.

Spectroscopically, the LP can hardly be detected in spectra near zenith at Korenica site, is dominant at Merenje site, as already described in section 3.2., and very strong at Zagreb site. The strength of individual LP lines can vary from site to site, depending on the relative numbers and types of different lamps that produce the LP, but, generally is dominated by natrium HP lamp spectra at all sites.

4. Conclusion

All-sky images of a moderately polluted sky confirm that light pollution is less severe in the infrared, and that LP growth towards the horizon is a little slower than in the visible. Similar results were obtained on different nights and on several locations with the approximately the same level of light pollution. In all cases, the main sources of light pollution were predominantly high-pressure sodium lamps.

Measurements carried out with modified SQM-L instrument show faster increase of light-pollution towards the horizon than data derived from all-sky images. This is attributed to relatively large acceptance angle of the SQM-L, compared to angular pixel size of the all-sky image. In SQM-L measurements the brighter sky in the lower part of the entrance cone contributes more to the total amount of radiation measured, resulting in apparently brighter sky. This is supported by the fact that this discrepancy becomes apparent at large zenith angles. The slower increase of the sky brightness in the infrared is also seen, although the angular resolution is too coarse for exact results.

The low dispersion spectra of the light polluted sky near zenith closely resemble the spectrum of HP sodium lamps. This type of lamps is dominant in the public lighting around the sites studied. The visible spectrum is dominated by pressure broadened sodium D doublet, with the characteristic self-absorption at 589 nm, and several lines between 500 and 570 nm. The near-infrared part of the spectrum shows only the very strong sodium doublet at 818.3 and 819.5 nm. This line doublet can easily be filtered out, or observations can be made on the long wavelength side of this doublet.

However, this can change in the future, as metal-halide lamps are replacing high-pressure sodium lamps in public lighting systems. They have complex spectra with a lot of lines, which vary considerably between particular lamp types. This can worsen the problem of light pollution, especially in the infrared, as there will be no easy way to filter it out anymore. If and when the LED sources are introduced massively into public lighting systems, the LP in the infrared would be greatly reduced as LEDs do not produce any emissions in the NIR. However, currently used LEDs produce excessive amounts of blue light that would wreak havoc in the visible, increasing LP levels in the visible drastically.

Acknowledgements – This work was partially supported by the Ministry of science, education and sports of the Republic of Croatia (scientific projects № 0195052 and 195-0000000-2233). One of the authors (Ž. A.) acknowledges support by the Alexander von Humboldt-Stiftung.

References

Albers, S. and Duriscoe, D. (2001): Modeling light pollution from population data and implications for national park service lands, *The George Wright Forum*, 18, 56–68.

ASTM (2011): American Society for Testing and Materials (ASTM) Terrestrial reference spectra for photovoltaic performance evaluation, http://rredc.nrel.gov/solar/spectra/am1.5/, accessed 22.04.2011.

Baader (2010a): http://www.teleskop-express.de/shop/product_info.php/info/p255_ACF-Astrofoto-Umbaufilter-fuer-Canon-EOS-300.html, accessed 21.04.2011.

Baader (2010b): http://astrosurf.com/buil/baader/evalÐ_us.htm, accessed 22.04.2011.

Bortle, J. E. (2001): Introducing the Bortle dark-sky scale, *Sky Telescope*, 101, 126–129.

Cinzano, P. (2005): Night Sky Photometry with Sky Quality Meter, ISTIL international report n. 9, v.1.4 2005, available at: http://www.unihedron.com/projects/darksky/sqmreport_v1p4.pdf, accessed 21.04.2011.

Duriscoe, D. M., Luginbuhl, C. B. and Moore, C. A. (2007): Measuring night-sky brightness with a wide-field CCD Camera, *Publ. Astron. Soc. Pac.*, 119,192–213.

Falchi, F. (2011): Campaign of sky brightness and extinction measurements using a portable CCD camera, *Mon. Not. R. Astron. Soc.*, 412, 33–48.

IAU (2012): http://www.iau.org/public/light_pollution/, accessed 02.05.2012.

IRIS (2010): Free software package IRIS, http://www.astrosurf.com/buil/us/iris/iris.htm, accessed 21.04.2011.

Ivezić, Ž. (2011): Private communication.

Marumi (2010): Marumi UV/IR cut filter, the spectral transmission curve is supplied with the filter. The transmission curve is almost rectangular, transmitting more than 95% between 380 and 700 nm, and almost nothing outside this spectral interval.

Patat, F. (2003): UBVRI night sky brightness during sunspot maximum at ESO-Paranal, *Astron. Astrophys.*, 400, 1183–1198.

RCA (1978): *RCA electro-optics handbook (second edition).* RCA Corporation, USA, 85 pp.

Schott (2010): Catalogue of Schott filter glasses, http://www.schott.com/advanced_optics/english/filter/index.html, accessed 21.04.2011.

Šegota, T. and A. Filipčić (2003): Köppenova podjela klima i hrvatsko nazivlje, *Geoadria*, 8, 17–37. (in Croatian, with English summary and figure captions)

Unihedron (2010a): http://unihedron.com/projects/sqm-l/, accessed 22.04.2011.

Unihedron (2010b): http://unihedron.com/projects/darksky/, accessed 22.04.2011.

Walker, A. and Schwarz, H. E. (2007): Night sky brightness at Cerro Pachon, Cerro Tololo Inter-American Observatory, http://www.ctio.noao.edu/site/pachon_sky/, accessed 21.04.2011.

Wiki (2011): http://unihedron.com/projects/darksky/ accessed 21.04.2011 http://en.wikipedia.org/wiki/KÐ%C3Ð%B6ppen_climate_classification

Zenit (2010): Page with the specifications of Peleng fish-eye objective, http://www.zenit-camera.com/canon-peleng-built-in-fisheye-lens.htm, accessed 22.04.2011.

SAŽETAK

Mjerenja svjetlosnog onečišćenja u bliskom infracrvenom području na hrvatskim lokacijama

Željko Andreić, Doroteja Andreić i Krešimir Pavlić

Opisana su istraživanja svjetlosnog onečišćenja u bliskom infracrvenom dijelu elektromagnetnog spektra (700–1000 nm) za lokacije na malim nadmorskim visinama, što je tipično za male zvjezdarnice u ovom području. Mjerenja pokazuju da je i u bliskom infracrvenom području prisutno znatno svjetlosno onečišćenje. Porast svjetline neba od zenita prema obzoru često je puta nešto sporiji u infracrvenom nego u vidljivom. U slučajevima kada je svjetlosno onečišćenje u najvećoj mjeri uzrokovano visokotlačnim natrijevim žaruljama, infracrvenim dijelom svjetlosnog onečišćenja dominiraju dvije bliske natrijeve linije (818,3 i 819,5 nm) koje se lako mogu ukloniti odgovarajućim fiterom. To se može promijeniti u budućnosti jer se natrijeve žarulje postupno zamjenjuju metal-halidnim žaruljama čiji spektri su složeni, i sastoje se od mnoštva linija u cijelom vidljivom i infracrvenom dijelu spektra.

Ako se u budućnosti dogodi prelazak na LED izvore svjetla, svjetlosno onečišćenje u infracrvenom dijelu spektra bit će znatno smanjeno. I na kraju, zbog male nadmorske visine opažačkih lokacija, i klimatskih svojstava područja u kojem se one nalaze, u atmos-

feri je prisutno mnogo više vlage i aerosola nego što je slučaj na planinskim zvjezdarnicama. Ova činjenica u kombinaciji s blizinom izvora svjetlosnog onečišćenja dovodi do pojačavanja svjetlosnog onečišćenja u usporedbi s uvjetima čiste i suhe atmosfere tipične za planinske zvjezdarnice.

Ključne riječi: svjetlosno onečišćenje, infracrveno: općenito

Corresponding author's address: Željko Andreić, University of Zagreb, Faculty of Mining, Geology and Petroleum Engineering, Pierottijeva 6, 10 000 Zagreb, Croatia, tel.: +385 (0)1 5535 920, e-mail: zandreic@rgn.hr